Evolutionary optimized discrete Tchebichef moments for image compression applications

Abdul Hameed RAGAMATHUNISA BEGUM[1,*]**, Duraisamy MANIMEGALI**[1]**,**
Ameerbasha ABUDHAHIR[2]**, Subramanian BASKAR**[3]

[1]Department of Information Technology, National Engineering College, Kovilpatti, Tamil Nadu, India
[2]Department of Electronics and Instrumentation Engineering, National Engineering College, Kovilpatti,
Tamil Nadu, India
[3]Department of Electrical and Electronics Engineering, Thiagarajar College of Engineering, Madurai,
Tamil Nadu, India

Abstract: Evolutionary optimized coefficients of discrete orthogonal Tchebichef moment transform (TMT) are utilized in this study to ameliorate the quality of the traditional moments-based image compression methods. Most of the existing methods compute moment-transform coefficients for the input image and then select the coefficients sequentially downward to a certain order based on the desired compression ratio. However, the proposed method divides the input image into nonoverlapping square blocks of specific size in order to circumvent the problem of numerical instability and then computes the TMT coefficients for each block. In this work, a real-coded genetic algorithm is employed to optimize the TMT coefficients of each block, which produces reconstructed images of better quality for the desired compression ratio. Here the optimization is carried out by minimizing the mean square error function. Standard test images of two different sizes (128×128 and 256×256) have been subjected to the proposed compression method for the block sizes (4×4 and 8×8) in order to assess its performance. The results reveal that the proposed real-coded genetic algorithm-based method outperforms others, namely the conventional sequential selection method and simple random optimization method, for the chosen input images in terms of the task of compression.

Key words: Image compression, Tchebichef moments, evolutionary optimization, real-coded genetic algorithm

1. Introduction

Satellite images, medical images, multimedia images, nondestructive testing images, etc. require huge memory and a higher bandwidth channel for their storage and transmission, respectively. However, these problems can certainly be minimized by compressing those images by means of suitable techniques without much compromising of their information and visual quality. In the past two decades, many researchers have reported quite a few compression techniques for binary, gray, and color still images, as well as for video images [1–3]. Different transforms and statistical methods have long been employed in developing more and more efficient image compression algorithms.

In the past, geometric and orthogonal moment functions were employed for various applications of image processing, which include image segmentation, computer vision, image analysis, and image compression [4–10]. Moments are derived from polynomial functions and computed for a digital image. They are statistical

---

*Correspondence: ahragamathunisabegum@yahoo.com

values that represent both low frequency information and high frequency details of an image. Unlike geometric moments, orthogonal moments, represent independent features of the image and thus have near zero or very minimum information redundancy in a set. The invariant property of orthogonal moments with respect to image translation, rotation, and sizing invites scientists/researchers to make use of them for various image processing applications [11–13]. Since continuous moments suffer from discretization error severely when they are numerically implemented in the domain of the discretized image coordinate space, few orthogonal polynomials/moments were directly defined in the discrete domain [14–18]. It has been well proven that the discrete orthogonal moments are very useful as pattern features in the analysis of two-dimensional images.

A general form for Krawtchouk, Charlier, Tchebichef, Mexiner, and Hahn moments was proposed by Zhu et al. recently [19]. Of the three moments, namely Tchebichef, Krawtchouk, and Hahn, considered in for their study for the task of compression, the Tchebichef outperformed others by reaching the highest value of peak-signal-to-noise ratio (PSNR), and the Hahn performed second best. To achieve the desired compression ratio, Zhu et al. arranged the absolute value of all moment values in a downward order and chose a part of them to reconstruct the image. This work aimed to build a simple compression method with better performance. The discrete orthogonal Tchebichef moment is considered in this study as its compression efficiency has already been proven [14,19,20].

A simple evolutionary optimization technique, the real-coded genetic algorithm (RGA), has been employed in this present work to choose the Tchebichef moment transform (TMT) coefficients required for reconstruction [21]. Different classes of benchmark images of various sizes are subjected to the proposed compression scheme in order to assess its performance. The results of the RGA-optimized-moment-based compression method reveal that the statistical quality measures computed for the reconstructed images are far better than that of other reported methods [19,22–24].

2. Theory of proposed compression method

The overall schematic diagram of the proposed compression method is shown in Figure 1. Before the compression process is instigated, the nonsquare input image is resized into the nearest possible square by replicating the required number of additional rows and columns in such a way that the resulting size (N × N) should be an integral multiple of the block size (n × n) for further processing. Based on the input block size, the resized image is divided into nonoverlapping square blocks of size n × n. Orthogonal discrete coefficients of TMT are then computed for each block up to the maximum possible order, i.e. n + n. Optimum TMT coefficients that contribute significantly for better quality of the reconstructed image are selected by minimizing the objective function, the so-called mean square error (MSE) function, using the RGA. A compressed image is then obtained by concatenating the optimal blocks horizontally, and then vertically. If the pixel intensity values of the original and reconstructed image block of size n × n are denoted as $g_b(u,v)$ and $\tilde{g}_b(u,v)$, respectively, the MSE is computed using Eq. (1).

$$MSE = \frac{1}{n^2} \sum_{u=0}^{n-1} \sum_{v=0}^{n-1} (g_b(u,v) - \tilde{g}_b(u,v))^2 \tag{1}$$

During the decompression process, the compressed image is divided into nonoverlapping square blocks in the same way as in the compression process. Subsequently, the inverse orthogonal discrete moment transform is performed for each block. Finally, an image of the original size (N × N) is simply constructed by concatenating the inversely transformed blocks horizontally and then vertically.
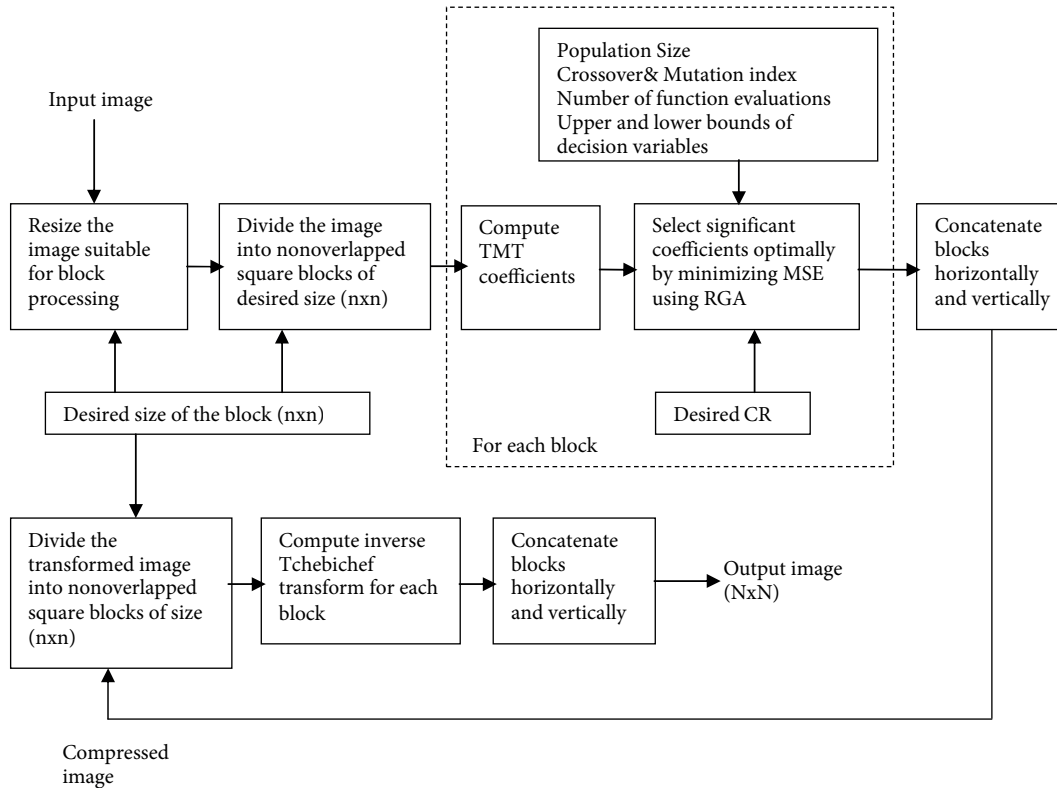
Figure 1. Schematic diagram of proposed TMT–RGA-based compression method.

3. Computation of 2-D discrete orthogonal Tchebichef moment

While the Tchebichef moments are directly defined in the discrete domain, computation of them for higher orders, particularly for large images, causes a numerical instability problem, which certainly affects the quality of the reconstructed image to a significant extent. This instability problem has been circumvented by computing the Tchebichef polynomial using the scaled-squared norm recurrence equations proposed by Mukundan [14,15]. For an image intensity distribution $g(u, v)$ of an image of size N $\times$ N, the coefficients of $i + j$ order TMT are computed from the scaled orthogonal Tchebichef polynomials $t_i(u)$ and $t_j(v)$ as:

$$T_{ij} = \frac{1}{\varphi(i, N)\varphi(j, N)} \sum_{u=0}^{N-1} \sum_{v=0}^{N-1} t_i(u)t_j(v)g(u, v) \quad i, j = 0, 1, 2, \ldots N\text{-}1. \tag{2}$$

The inverse moment transform for the exact reconstruction of the image is:

$$g(u, v) = \sum_{i=0}^{N-1} \sum_{j=0}^{N-1} T_{ij}t_i(u)t_j(v) \quad u, v = 0, 1, 2, \ldots N\text{-}1, \tag{3}$$

where:

$$t_i(u) = \frac{(2i - 1)t_1(u)t_{i-1}(u) - (i - 1)\left(1 - \frac{(i-1)^2}{N^2}\right)t_{i-2}(u)}{i} \tag{4}$$

where $i = 2,3,4,\ldots N\text{-}1$.

Similarly, $t_j(v)$ can be obtained from Eq. (4) by replacing the variables appropriately. The polynomials $t_i(u)$ and $t_j(v)$ in Eq. (2) satisfy the recurrence formula given in Eq. (4). The initial conditions are given in Eq. (5).

$$t_o(u) = t_o(v) = 1$$
$$t_1(u) = \frac{(2u-N+1)}{N} \text{ and } t_1(v) = \frac{(2v-N+1)}{N} \tag{5}$$

The squared-norm $\phi(i, N)$ in Eq. (2) is expressed by:

$$\phi(i, N) = \frac{N \left(1 - \frac{1}{N^2}\right) \left(1 - \frac{2^2}{N^2}\right) \cdots \left(1 - \frac{i^2}{N^2}\right)}{2i+1} \tag{6}$$

$i = $ 0,1,2,... N-1.

Similarly, $\phi(j, N)$ in (2) can be obtained from Eq. (6) by replacing the variables appropriately.

For better compression applications, the Tchebichef moments T_{ij} are optimized for the given compression ratio by minimizing the MSE function using the RGA. The optimal Tchebichef moments are here denoted as T_{pq}^{opt}. The pixel intensity values of the reconstructed image are obtained from T_{pq}^{opt} using Eq. (7).

$$\tilde{g}(u, v) = \sum_{i=0}^{N-1} \sum_{j=0}^{N-1} T_{ij}^{opt} t_i(u) t_j(v) \tag{7}$$

4. Proposed compression algorithm

Figure 2 shows the flowchart of the proposed compression algorithm, which is explained as follows. The image of size N × N that is to be compressed is input. The desired compression ratio (CR), the block size (n × n), and the number of iterations are keyed in. The image is divided into nonoverlapping blocks of size n × n. The pixel intensity values of a block are denoted as $g_b(u, v)$. The required number of coefficients (RNC) that are to be selected from each block is calculated using Eq. (8).

$$RNC = Round \left\{ \left(1 - \frac{CR}{100}\right) \times n^2 \right\} \tag{8}$$

Then the Tchebichef polynomials $t_i(u)$ and $t_j(v)$ and square-norm $\varphi(i, N)$ and $\varphi(j, N)$ are computed for a block of size (n × n) using Eqs. (4), (5), and (6). The blocks are processed horizontally from the topmost-left one. The Tchebichef coefficients are computed using Eq. (2) for each block. Numbers of row and column blocks are represented as NRB and NCB, respectively, and are determined by dividing the size of the square image (N) by the size of the square block (n). The RNC is selected from each block using the RGA, the process of which is discussed in detail in the next section. The optimal Tchebichef coefficients are denoted as T_{ij}^{opt}. The selection of coefficients by the RGA is shown using the subprogram symbol in the flowchart. Concatenation of blocks with optimal coefficients is done horizontally and then vertically in order to represent the input image in the transformed-compressed domain. During the process of decompression, the compressed image is again block-processed, and then inverse TMT is performed for each block. Finally, the decompressed image of size N × N is displayed by concatenating the blocks horizontally and vertically.

5. Selection of optimum TMT coefficients

As the moments based on discrete polynomials exhibit a reasonable energy compaction for quite a few classes of images, they are generally used for image compression applications. Conventionally, the TMT coefficients are chosen sequentially downward to a certain order, based on the desired compression ratio. In general, it was felt that only a few coefficients of moment transform yield a very high compression ratio and vice versa by sacrificing the quality of reconstructed images [19]. However, if optimum coefficients are properly chosen, most of the energy in an image will be concentrated on a relatively small number of moment transform coefficients. Various components of the RGA are briefly explained in Section 5.1 as employed in this work to choose the optimum TMT coefficients.

5.1. Real-coded genetic algorithm (RGA)

As the GA considers multiple points simultaneously during a genetic search, the chance of being trapped in the local optimum is much less [25,26]. The generalized steps involved in a common optimization task using the GA are as follows: 1) Possible solutions to the given problem are represented genetically. 2) Population of solutions is created using an appropriate technique. 3) Fitness of the solution is rated using an evaluation function. 4) During the process of reproduction, the genetic composition of the children that will be the parents for the next generation is altered by parent selection mechanism and genetic operators. 5) Parameter values required for the genetic algorithm are set specifically.

It has been well proven that for most of the constrained optimization problems, real-number encoding yields the best performance in the sense that it always outperforms gray and binary encoding. Simulated binary (SBX) crossover and nonuniform polynomial mutation considered for the reproduction process are adaptive and are described in the following subsections [27,28].

6. Simulated binary crossover

Creation of two-offspring solutions from two parents in SBX crossover is achieved through the following equations.

$$\beta_{qk} = \begin{cases} (2m_k)^{\frac{1}{\eta_c+1}}, & m_k \leq 0.5 \\ \\ \left(\frac{1}{2(1-m_k)}\right)^{\frac{1}{\eta_c+1}}, & \text{otherwise} \end{cases} \tag{9}$$

Here, m_k is a chosen random number in the interval $[0,1]$, and β_{qk} and η_c are a spread factor and the crossover index respectively. Eq. (10) computes the offspring $z_k^{(1,h+1)}$ and $z_k^{(2,h+1)}$.

$$\begin{aligned} z_k^{(1,h+1)} &= 0.5\left[(1+\beta_{qk})z_k^{(1,h)} + (1-\beta_{qk})z_k^{(2,h)}\right] \\ z_k^{(2,h+1)} &= 0.5\left[(1-\beta_{qk})z_k^{(1,h)} + (1+\beta_{qk})z_k^{(2,h)}\right] \end{aligned} \tag{10}$$

7. Nonuniform polynomial mutation

Subsequent to SBX operation, a polynomial mutation operation is performed to generate new offspring using the probability distribution function. If z_k^U is the upper and z_k^L is the lower limit value, the new offspring $y_k^{(1,h+1)}$ is derived using Eq. (11).

$$y_k^{(1,h+1)} = z_k^{(1,h+1)} + (z_k^U - z_k^L)\overline{\delta_k} \tag{11}$$
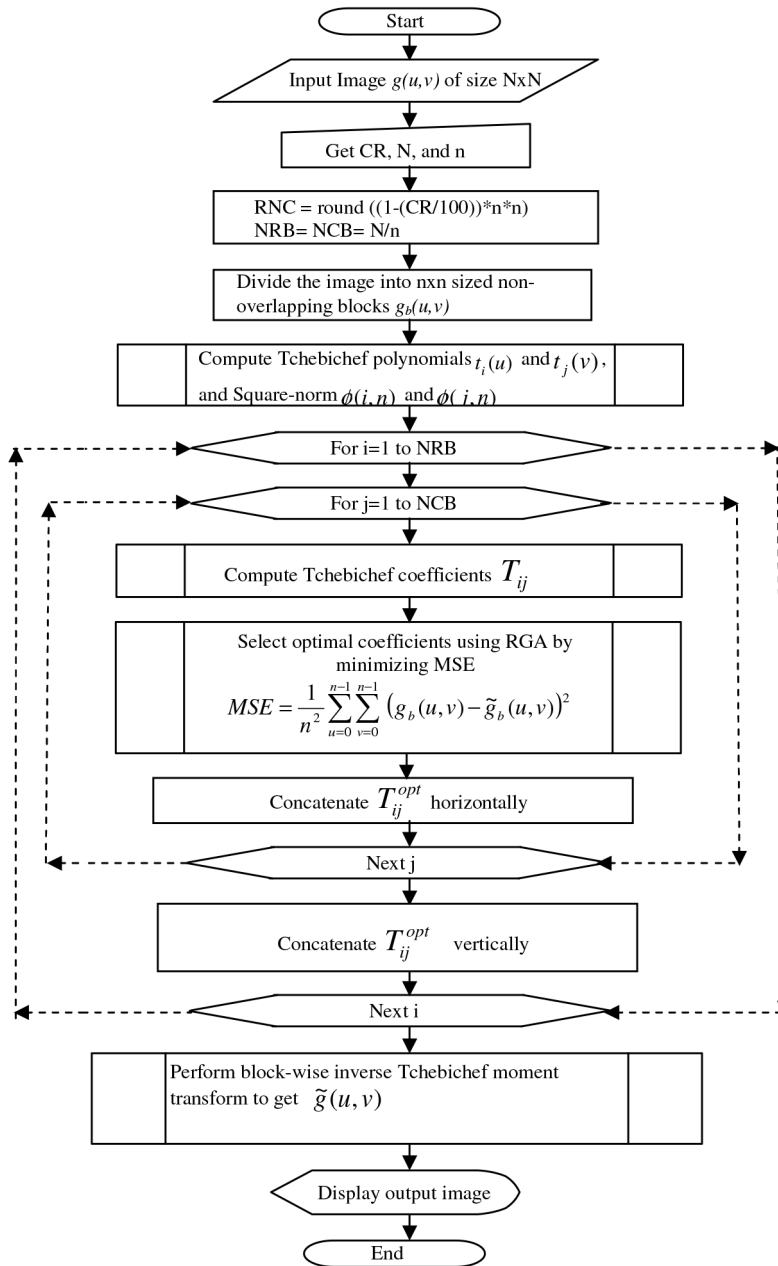
Figure 2. Flowchart of the proposed RGA-based compression algorithm.

Eq. (12) computes the parameter $\overline{\delta_k}$ from $P(\delta)$.

$$P(\delta) = 0.5(\eta_m + 1)\, (1 - |\delta|)^{\eta_m}$$

$$\overline{\delta_i} = \begin{cases} (2v_k)^{1/(\eta_m+1)} - 1, if v_k < 0.5 \\ 1 - [2(1 - v_k)]^{1/(\eta_m+1)}, \ if v_k \geq 0.5 \end{cases} \tag{12}$$

Here, η_m is the mutation index.

Parents are replaced by the newly generated offspring that become the population members for the subsequent generation. These steps are repeated until the specified stopping criterion is satisfied.

7.1. Selection of optimum TMT coefficients using RGA

The following steps are an elaborate description of the RGA-based procedure for selecting optimum coefficients of TMT in order to yield a better quality reconstructed image without sacrificing the compression ratio.

Step 1: Input the desired compression ratio and block size.

Step 2: Calculate RNCs using Eq. (8).

Step 3: Compute TMT coefficients using Eq. (1) for a chosen block ($g_b(u,v)$) of size n $\times$ n.

Step 4: Set the parameters required for genetic algorithm as follows. Number of variables to be optimized = RNC, Number of runs = 10; Penalty factor = 1000; Lower bound value of the variables = 1; Upper bound value of the variables = n^2; Maximum number of function evaluations = 10,000; Population size = RNC $\times$ 10; Crossover probability = 0.8; SBX crossover index = 5; Mutation index = 20; Mutation probability = 1/RNC.

Step 5: Create initial population of solutions.

Step 6: Evaluate the value of fitness function using the following steps.

Step 7: Sort the individuals (optimum locations) in an ascending order.

Step 8: Create an array of size 1 $\times$ n^2 with all zeros.

Step 9: Replace the zeros in the above array by '1' where the index of zeros equals the optimum locations in the sorted array.

Step 10: Convert the resulted one-dimensional array of size 1 $\times$ n^2 into a two-dimensional array of size n $\times$ n so-called window.

Step 11: Perform element-by-element multiplication between the window and the block of TMT coefficients.

Step 12: Select parents required for reproduction using tournament selection mechanism.

Step 13: Perform SBX crossover between the selected parents and apply polynomial mutation in order to produce children that are the population for the next generation.

Step 14: Repeat steps 6–13 until the maximum number of function evaluations is completed.

Step 15: Perform inverse TMT using Eq. (7) to get $\tilde{g}_b(u,v)$.

Step 16: Repeat steps 3 to 15 for the subsequent blocks.

8. Results and discussion

Various benchmark images of different sizes were subjected to the proposed compression method to prove its performance. The images, namely Lena and Baboon of size 128 $\times$ 128 and Lady and House of size 256 $\times$ 256, are considered in this study. These images were obtained from the University of Southern California Signal and Image Processing Institute (USC-SIPI) [29]. The quality measures that numerically quantify the fidelity of the reconstructed image, MSE and PSNR (dB), are computed using Eqs. (13) and (14), respectively, for three different compression ratios (50%, 75%, and 87.5%) in order to precisely assess the performance of the proposed method.

$$MSE = \frac{1}{N^2} \sum_{u=0}^{N-1} \sum_{v=0}^{N-1} (g(u,v) - \tilde{g}(u,v))^2 \tag{13}$$

$$PSNR(dB) = 10\log_{10}\left[\dfrac{255^2}{\frac{1}{N^2}\sum\limits_{u=0}^{N-1}\sum\limits_{v=0}^{N-1}\left(g(u,v) - \tilde{g}(u,v)\right)^2}\right] \tag{14}$$

To find the optimal TMT coefficients of the chosen block, the RGA-based optimization method is employed owing to its simplicity and effectiveness. The number of iterations required for the algorithm is set as 10. In order to compare the performance of the proposed evolutionary selection method (ESM) on the compression application, the sequential selection method (SSM) [19] and random selection method (RSM) [24] have been considered. MATLAB codes were developed for the proposed algorithm and executed. To prove the consistency of the RGA, for each block of the input image, the optimal moment coefficients were selected from the best 10 independent trials.

Having chosen the block size as 4 × 4 and 8 × 8, the performance measures were computed for both the algorithms. The results are given in Tables 1 and 2, respectively, for all the chosen images of size 128 × 128 and 256 × 256. The MSE and PSNR values indicate that the proposed algorithm performs better than the sequential selection algorithm and random optimization method. The ability of the presented algorithm is high in selecting optimum moment transform coefficients as compared to the other methods irrespective of the size of the images and block size chosen.

Table 1. Results of proposed algorithm and recently reported methods for the images of size 128 × 128.

Image size 128 × 128								
Block size			4 × 4			8 × 8		
CR (%)			50	75	87.5	50	75	87.5
SSM	Lena	MSE	23.94	86.93	115.83	21.96	74.50	177.16
		PSNR (dB)	34.33	28.74	27.49	34.71	29.41	25.65
	Baboon	MSE	25.33	67.04	79.09	24.10	62.26	111.07
		PSNR (dB)	34.10	29.87	29.15	34.31	30.19	27.68
RSM [24]	Lena	MSE	13.36	49.96	102.61	36.29	100.23	172.22
		PSNR (dB)	36.87	31.14	28.02	32.53	28.12	25.77
	Baboon	MSE	9.19	31.03	58.89	58.89	23.19	57.37
		PSNR (dB)	38.50	33.21	30.43	30.43	34.48	30.54
ESM	Lena	MSE	5.38	30.16	91.19	12.21	24.98	55.07
		PSNR (dB)	40.82	33.34	28.53	37.27	34.16	30.72
	Baboon	MSE	4.44	20.54	52.94	9.98	18.20	36.46
		PSNR (dB)	41.66	35.01	30.89	38.14	35.53	32.51

Though the sequential selection method and random optimization method had shorter computation time, they may perhaps lack the ability of minimizing the MSE to the level attained by the proposed RGA based technique. Since the optimization was not carried out online, the proposed method is not sluggish in relation to the task of selecting the optimal TMT coefficients.

The reconstructed images of various sizes of the proposed method and sequential selection method are shown in Figures 3 and 4.
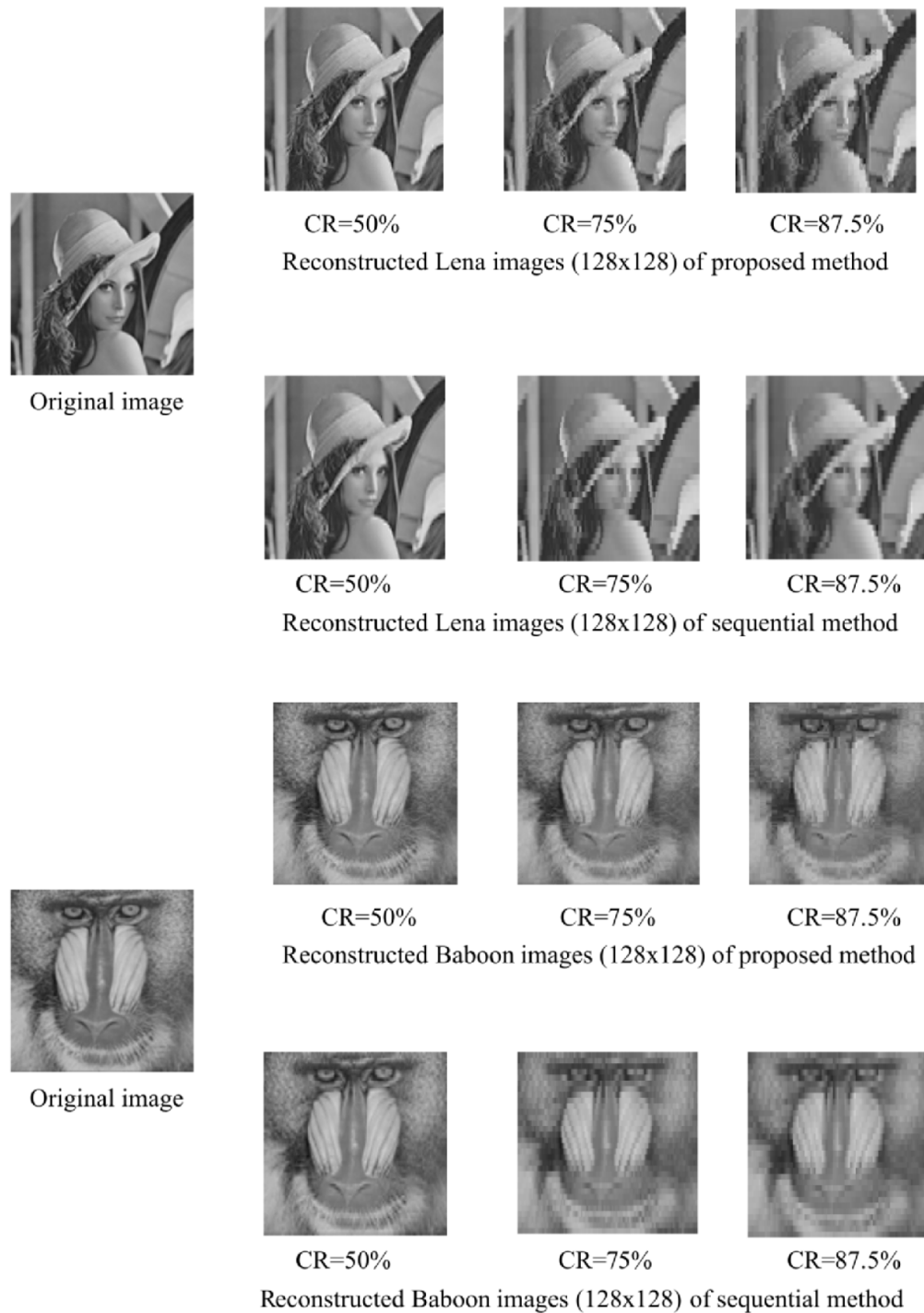
Figure 3. Reconstructed Lena and Baboon images (128 × 128) of proposed and sequential methods for the block size 4 × 4.

In spite of the fact that all the methods indeed compress the input images to a desirable extent, both the visual quality of the images shown in Figures 3 and 4 and the performance measures given in Tables 1 and 2 strongly confirm that the proposed algorithm outperforms the sequential selection-based method and random

selection method for all the chosen images. The percentage reduction in the MSE and percentage increase in the PSNR values, computed using Eqs. (15) and (16), of the proposed method over the other methods are given in Tables 3 and 4, respectively. This substantial reduction in MSE and the appreciable increase in the PSNR values certainly show that the proposed method globally ameliorates the quality of the reconstructed images for the compression ratios of 50%, 75%, and 87.5%.
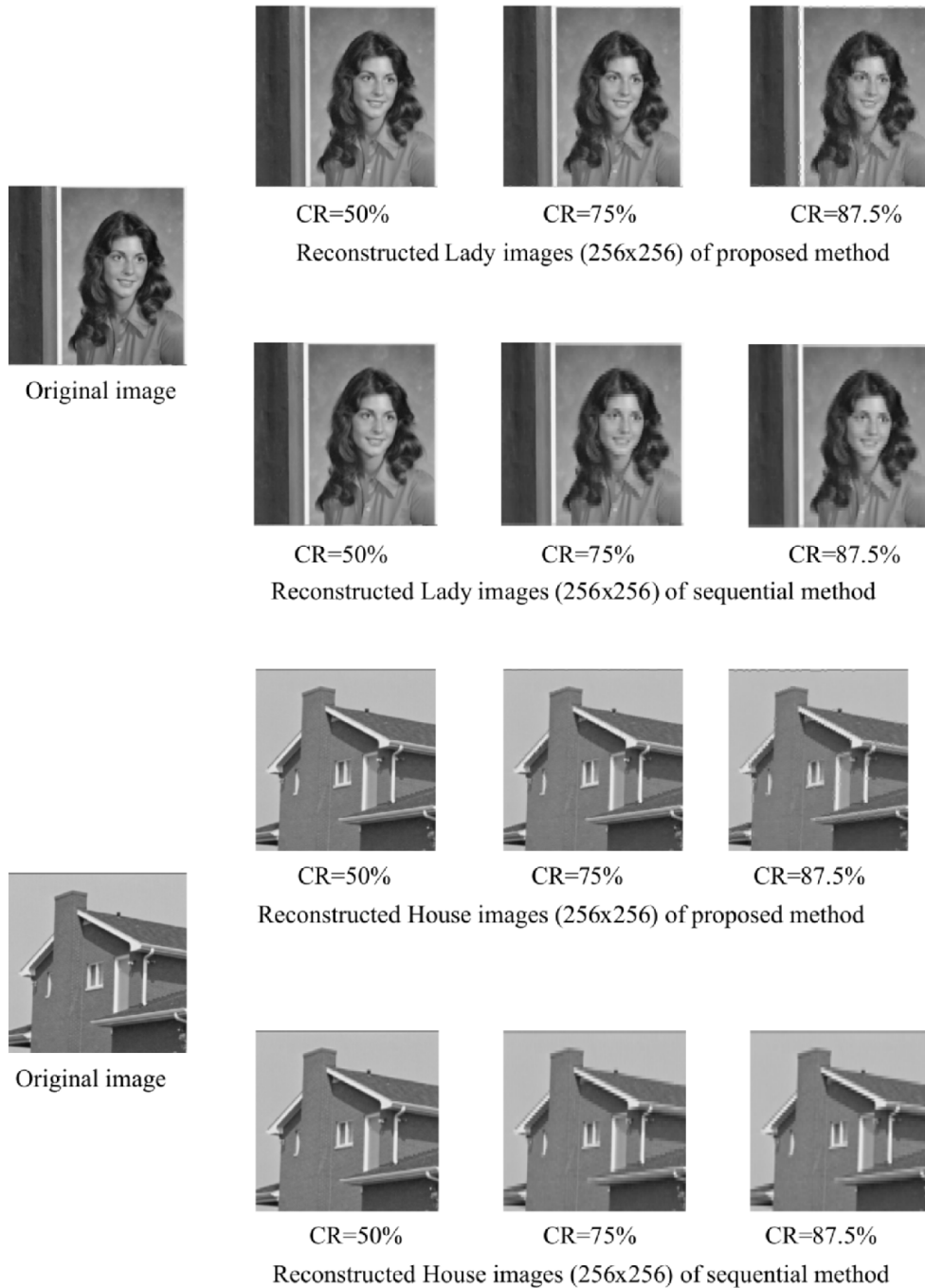

Figure 4. Reconstructed Lady and House images (256 × 256) of proposed and sequential methods for the block size 4 × 4.

Table 2. Results of proposed algorithm and recently reported methods for the images of size 256 × 256.

Image size 256 × 256								
Block size			4 × 4			8 × 8		
CR (%)			50	75	87.5	50	75	87.5
SSM	Lady	MSE	7.30	30.67	39.35	5.65	21.71	85.71
		PSNR (dB)	39.50	33.26	32.18	40.61	34.76	28.80
	House	MSE	22.79	61.60	67.54	16.02	53.59	119.41
		PSNR (dB)	34.55	30.23	29.84	36.08	30.84	27.36
RSM [24]	Lady	MSE	1.51	9.07	30.98	5.38	25.66	62.71
		PSNR (dB)	46.35	38.55	33.22	40.82	34.04	30.16
	House	MSE	2.37	14.98	43.19	8.68	37.75	69.12
		PSNR (dB)	44.39	36.38	31.78	38.75	32.36	29.73
ESM	Lady	MSE	0.67	3.72	21.72	1.61	3.20	7.71
		PSNR (dB)	49.87	42.43	34.76	46.05	43.09	39.26
	House	MSE	0.87	6.31	34.88	2.24	4.55	12.26
		PSNR (dB)	48.72	40.13	32.71	44.64	41.55	37.25

Table 3. Percentage reduction in the MSE of the proposed method over the other methods.

Block size	CR (%)	Percentage reduction in the MSE of ESM							
		Over SSM				Over RSM [24]			
		128 × 128		256 × 256		128 × 128		256 × 256	
		Lena	Baboon	Lady	House	Lena	Baboon	Lady	House
4 × 4	50	77.53	82.47	90.82	96.18	59.73	51.69	55.63	63.29
	75	65.31	69.36	87.87	89.76	39.63	33.81	58.99	57.88
	87.5	21.27	33.06	44.80	48.36	11.13	10.10	29.89	19.24
8 × 8	50	44.40	58.59	71.50	86.02	66.35	83.05	70.07	74.19
	75	66.47	70.77	85.26	91.51	75.08	21.52	87.53	87.95
	87.5	68.92	67.17	91.01	89.73	68.02	36.45	87.71	82.26

Table 4. Percentage increase in the PSNR of the proposed method over the other methods.

Block size	CR (%)	Percentage increase in the PSNR of ESM							
		Over SSM				Over RSM [24]			
		128 × 128		256 × 256		128 × 128		256 × 256	
		Lena	Baboon	Lady	House	Lena	Baboon	Lady	House
4 × 4	50	15.90	18.15	20.79	29.09	9.68	7.59	7.06	8.89
	75	13.80	14.68	21.61	24.67	6.60	5.14	9.15	9.35
	87.5	3.65	5.63	7.42	8.77	1.79	1.49	4.43	2.84
8 × 8	50	6.87	10.04	11.81	19.18	12.72	20.22	11.36	13.19
	75	13.91	15.03	19.33	25.78	17.68	2.96	21.00	22.12
	87.5	16.50	14.86	26.64	26.55	16.11	6.06	23.18	20.19

$$Percentage reduction in MSE = \frac{MSE(othermehod) - MSE(proposed)}{MSE(othermehod)} \times 100 \qquad (15)$$

$$Percentage increase in PSNR = \frac{PSNR(proposed) - PSNR(othermehod)}{PSNR(proposed)} \times 100 \qquad (16)$$

The quality measure that portrays human visual perception, the mean structural similarity (MSSIM) index, has also been computed using the algorithm given in [30] for the three methods, namely SSM, RSM, and ESM,

and is given in Table 5. It is observed that the standard conventional metrics such as MSE and PSNR are also inconsistent with the MSSIM for assessing the image quality information. The computed values of MSSIM revealed that the proposed method outperforms others for different block sizes and compression ratios.

Table 5. A comparison of MSSIM of the proposed method over the reported methods.

Image	Block size	MSSIM								
		SSM			RSM [24]			ESM		
		Compression ratio (%)			Compression ratio (%)			Compression ratio (%)		
		50	75	50	50	75	87.5	50	75	87.5
Lena (128 × 128)	4	0.9505	0.8406	0.7778	0.9697	0.8975	0.7977	0.9861	0.9330	0.8232
	8	0.9013	0.7462	0.6201	0.9044	0.7792	0.6671	0.9625	0.9225	0.8554
Baboon (128 × 128)	4	0.9023	0.7355	0.6781	0.9609	0.8638	0.7129	0.9788	0.9050	0.7707
	8	0.9041	0.7451	0.5865	0.9011	0.7604	0.6277	0.9530	0.9084	0.8212
Lady (256 × 256)	4	0.9750	0.9167	0.8903	0.9881	0.9552	0.8952	0.9934	0.9721	0.9175
	8	0.9718	0.9216	0.8365	0.9650	0.8855	0.7972	0.9853	0.9728	0.9458
House (256 × 256)	4	0.9211	0.8321	0.8111	0.9834	0.9377	0.8711	0.9915	0.9597	0.8905
	8	0.9190	0.8284	0.7336	0.9507	0.8622	0.7934	0.9806	0.9633	0.9235

9. Conclusions

The evolutionary optimization-based compression scheme certainly improves the efficiency of the orthogonal moments-based conventional compression technique to a reasonable extent. The proposed algorithm that utilized optimally selected TMT coefficients was found to be quite suitable for the compression of varied sizes of images. Optimal TMT coefficients required for compressing the images, namely Lena, Baboon, Lady, and House, were obtained using the RGA. The proposed compression technique was simulated using MATLAB codes and it yielded satisfactory results. In this work, the RGA method for selecting optimum TMT coefficients does its job phenomenally by numerically minimizing the objective function. The results of the earlier reported methods of other researchers were compared with the results of the evolutionary-based compression method. It was well affirmed that for all the chosen images, the proposed compression method consistently produces better results than the TMT-based traditional compression methods reported by Zhu et al. and Abu et al. Also, the proposed evolutionary optimization-based method performs better than the random optimization method. The proposed compression algorithm will certainly save the memory requirement to a greater extent when multiple classes of images are stored and analyzed in a common image database. Since the basis functions of discrete TMT and discrete cosine transform are orthogonal, the former can be straightforwardly deployed instead of the latter in the JPEG baseline technique. In order to achieve improved compression performance of international compression standard JPEG, the 4 × 4 block TMT coefficients selected using the proposed method would be quantized and coded using Huffman tables as recommended in JPEG standards and then stored so that the header information during the compression process can be uniquely decoded during the decompression process. Appropriately incorporating the minimal changes in the present algorithm and using a multicore digital processor can offer an efficient online compression engine for multimedia applications. It is worth mentioning that this method is applicable not only to the images that were chosen in this study but also for others possessing wide spectral variations of any nature, and for any desired compression ratio. This method is inherently slow when compared with the sequential selection method conventionally employed for moments-based compression because, for the desired compression ratio, quite a few iterations are to be inevitably elapsed to select the optimum TMT coefficients from each block in order to have a higher value of the PSNR, but its simplicity, versatility, and effective compression ability will undoubtedly attract end-users. The use of high-

speed digital processors in a grid computing system to select the optimal TMT coefficients hopefully justifies the real-time implementation of the proposed compression method.

References

[1] Jain AK. Fundamentals of Digital Image Processing. Upper Saddle River, NJ, USA: Prentice Hall, 1989.

[2] Lazzerini B, Marcelloni F, Vecchio M. A multi-objective evolutionary approach to image quality/compression trade-off in JPEG baseline algorithm. Appl Soft Comput 2010; 10: 548-561.

[3] Ou YF, Ma Z, Liu T, Wang Y. Perceptual quality assessment of video artifacts. IEEE T Circ Syst Vid 2011; 21: 286-298.

[4] Teague MR. Image analysis via the general theory of moments. J Opt Soc Am 1980: 70: 920-930.

[5] Zenkouar H, Nachit A. Images compression using moments method of orthogonal polynomials. Mater Sci Eng B-Adv 1997; 49: 211-215.

[6] Yap PT, Paramesran R, Ong SH. Image analysis by Krawtchouk moments. IEEE T Image Process 2003; 12: 1367-1377.

[7] Chong CW, Raveendran P, Mukundan R. Translation and scale invariants of Legendre moments. Pattern Recogn 2004; 37: 119-129.

[8] Yap PT, Parmesran R, Ong SH. Image analysis using Hahn moments. IEEE T Pattern Anal 2007; 29: 2057-2062.

[9] Papakostas GA, Boutalis YS, Karras DA, Mertzios BG. Pattern classification by using improved wavelet compressed Zernike moments. Appl Math Comput 2009; 212: 162-176.

[10] Papakostas GA, Karakasis EG, Koulouriotis DE. Novel moment invariants for improved classification performance in computer vision applications. Pattern Recogn 2010; 43: 58-68.

[11] Mukundan R, Ramakrishnan KR. Moment Functions in Image Analysis – Theory and Applications. Singapore: World Scientific Publishing Company, 1998.

[12] Zhu H, Shu H, Xia T, Luo L, Coatrieux JL. Translation and scale invariants of Tchebichef moments. Pattern Recogn 2007; 40: 2530-2542.

[13] Belkasim SO, Shridhar M, Ahmadi M. Pattern recognition with moment invariants – a comparative study and new results. Pattern Recogn 1991; 24: 1117-1138.

[14] Mukundan R. Some computational aspects of discrete orthonormal moments. IEEE T Image Process 2004; 13: 1055-1059.

[15] Mukundan R, Ong SH, Lee PA. Image analysis by Tchebichef moments. IEEE T Image Process 2001; 10: 1357-1364.

[16] Mukundan R. Improving image reconstruction accuracy using discrete orthonormal moments. In: International Conference on Imaging Systems, Science and Technology; 23–26 June 2003; Las Vegas, NV, USA. pp. 287-293.

[17] Abu NA, Suryana N, Mukundan R. Perfect image reconstruction using discrete orthogonal moments. In: 4th IASTED International Conference on Visualization, Imaging, and Image Processing; 6–8 September 2004; Marbella, Spain. pp. 903–907.

[18] Hunt O, Mukundan R. A comparison of discrete orthogonal basis functions for image compression. In: Conference on Image and Vision Computing New Zealand; 21–23 November 2004; Akaroa, New Zealand. pp. 53-58.

[19] Zhu H, Liu M, Shu H, Zhang H, Luo L. General form for obtaining orthogonal moments. IET Image Process 2010; 4: 335-352.

[20] Nakagaki K, Mukundan R. A fast 4×4 forward discrete Tchebichef transform algorithm. IEEE Signal Proc Let 2007; 14: 684-687.

[21] Back T, Fogel DB, Michalewicz Z. Handbook of Evolutionary Computation. 1st ed. Bristol, UK: IOP Publishing Ltd., 2002.

[22] Lang WS, Abu NA, Rahmalan H. Fast 4×4 Tchebichef moment image compression. In: International Conference of Soft Computing and Pattern Recognition; 4–7 December 2009; Malacca, Malaysia. pp. 295–300.

[23] Abu NA, Wong SL, Herman NS Mukundan R. An efficient compact Tchebichef moment for image compression. In: 10th International Conference on Information Sciences, Signal Processing and their Applications; 10–13 May 2010; Kuala Lumpur, Malaysia. pp. 448-451.

[24] Ragamathunisa Begum AH, Manimegalai D, Abudhahir A. Optimum coefficients of discrete orthogonal Tchebichef moment transform to improve the performance of the image compression. Malayas J Comput Sci 2013; 26: 60-75.

[25] Kern S, Muller SD, Hansen N, Buche D, Ocenasek J, Koumoutsakos P. Learning probability distributions in continuous evolutionary algorithms-a comparative review. Nat Comp Ser 2004; 3: 77-112.

[26] Deb K, Kumar A. Real-coded genetic algorithms with simulated binary crossover: studies on multi-modal and multi-objective problems. Complex Syst 1995; 9: 431-454.

[27] Deb K. Multi-Objective Optimization Using Evolutionary Algorithms. Chichester, UK: John Wiley & Sons Ltd., 2001.

[28] Abudhahir A, Baskar S. An evolutionary optimized nonlinear function to improve the linearity of transducer characteristics. Meas Sci Technol 2008; 19: 045103.

[29] Signal and Image Processing Institute, University of Southern California. Database. Available online at http://sipi.usc.edu/database.

[30] Sheikh HR, Sabir MF, Bovik AC. A statistical evaluation of recent full reference image quality assessment algorithms. IEEE T Image Process 2006; 15: 3440-3451.